RESEARCH PAPER

In Vitro Evaluation of Clinical Candidates of γ-Secretase Inhibitors: Effects on Notch Inhibition and Promoting Beige Adipogenesis and Mitochondrial Biogenesis

Di Huang [1,2,3] • Jiamin Qiu [1] • Shihuan Kuang [1,4] • Meng Deng [2,3,5,6]

ABSTRACT

Purpose Inhibition of Notch signaling has been recently demonstrated to promote beige adipocyte biogenesis. However, most γ-secretase inhibitors (GSIs) used to achieve pharmacological inhibition of Notch signaling are at the basic research or preclinical stage, limiting the translation of fundamental findings into clinical practice. This present study aimed to evaluate the potential of several clinical candidates of GSIs as browning agents for the treatment of obesity.

Methods Seven GSIs that are clinical candidates for the treatment of Alzheimer's disease or cancer were selected and their impacts on Notch inhibition as well as promoting beige biogenesis were compared using *in vitro* culture of 3T3-L1 preadipocytes.

Results Four compounds (i.e.RO4929097, PF-03084014, LY3039478, and BMS-906024) that efficiently inhibited the expression of Notch target genes in 3T3-L1 preadipocytes were identified. Moreover, these compounds were optimized for dose-dependent effects at three gradient concentrations (0.5, 1, and 10 μM) to promote beige adipogenesis and mitochondrial biogenesis in 3T3-L1 preadipocytes without causing severe cytotoxicity.

Conclusions Our findings not only highlight the potential of cross-therapeutic application of these GSIs for obesity treatment via inhibition of γ-secretase-mediated processing of Notch signaling, but also provide important experimental evidence to support further design and development of clinically translatable Notch-inhibiting drug delivery systems.

KEY WORDS Obesity · Notch signaling pathway · γ-secretase inhibitor · Adipose browning · 3T3-L1 preadipocytes

✉ Shihuan Kuang
skuang@purdue.edu

✉ Meng Deng
deng65@purdue.edu

1   Department of Animal Sciences, Purdue University, West Lafayette, IN 47907, USA

2   Department of Agricultural and Biological Engineering, Purdue University, West Lafayette, IN 47907, USA

3   Bindley Bioscience Center, Purdue University, West Lafayette, IN 47907, USA

4   Center for Cancer Research, Purdue University, West Lafayette, IN 47907, USA

5   School of Materials Engineering, Purdue University, West Lafayette, IN 47907, USA

6   Weldon School of Biomedical Engineering, Purdue University, West Lafayette, IN 47907, USA

ABBREVIATIONS

BAT	Brown adipose tissues
C/EBPs	CCAAT/enhancer binding protein family proteins
CIDEA	Cell death-inducing DNA fragmentation factor alpha-like effector A
COX5B	Cytochrome c oxidase subunit 5B
DAPT	(N-[N-(3,5-Difluorophenacetyl)-l-alanyl]-S-phenylglycine t-butyl ester)
DIO2	Type 2 deiodinase
FABP4	Fatty acid binding protein 4
GSIs	γ-secretase inhibitors
NICD	Notch intracellular domain
PPARs	Peroxisomal proliferator-activated receptor family proteins

Published online: 04 September 2020

🌐 Springer

PPARGC1α	Peroxisome proliferator-activated receptor gamma coactivator 1-alpha
PRDM16	PR domain containing 16
RBPJ	Recombination signal binding protein for immunoglobulin kappa J region
TMEM26	Transmembrane protein 26
UCP1	Uncoupling protein 1
WAT	White adipose tissue

INTRODUCTION

Obesity is a chronic disease that is strongly associated with a reduction in life expectancy and an increase in mortality from cardiovascular disease, diabetes, cancer, and other causes. Current estimates show that over 50% of the world's population will be overweight or obese by the year 2030 if the trends continue [1]. Understanding the processes and metabolic perturbations that contribute to fat accumulations accompanying obesity is particularly important for the development of therapeutic strategies [2]. The expansion of white adipose tissue (WAT) contributes to insulin resistance and inflammation that may lead to type 2 diabetes. In contrast, brown adipocytes found in brown adipose tissues (BAT) can break down and utilize lipids to generate heat via uncoupling protein 1 (UCP1)-mediated thermogenesis, and BAT abundance is positively associated with systemic metabolic activity [3]. Thermogenic adipocytes called beige (or brite, for brown-in-white) adipocytes can also be found in certain WAT depots and their presence is dynamically regulated by intrinsic factors and external stimuli. Beige adipocytes can be transformed from white adipocytes through a process termed 'browning' or 'beiging'. Recent studies have shown that previously identified BAT deposits in adult humans are primarily composed of beige adipocytes, providing a foundation for studying adipose browning with therapeutic potential in the treatment of obesity [4, 5].

Notch signaling plays a critical role in development and regeneration of stem/progenitor cells as well as in regulation of cell fate [6]. It is known to be an evolutionarily conserved mechanism that balances differentiation and proliferation in several cell types, including muscle stem cells and adipocyte progenitor cells [7–9]. Notch signaling is mediated by binding of Delta-like and Serrate/Jagged family ligands with Notch receptors (Notch-1, −2, −3, and −4), leading to γ-secretase-mediated proteolytic cleavage and the release of Notch intracellular domain (NICD). Subsequently, NICD translocates to the nucleus, where it interacts with the recombination signal binding protein for immunoglobulin kappa J region (RBPJ) transcriptional complex to activate the transcription of downstream targets, including HES and HEY family genes, to regulate cell differentiation [10].

The process of adipogenesis includes five steps, which are cell proliferation, cell contact inhibition/growth arrest, clonal expansion, permanent growth arrest, and lipid accumulation [11]. The transcriptional control of adipogenesis involves the activation of several families of transcription factors, such as CCAAT/enhancer binding protein family proteins (C/EBPs) and peroxisomal proliferator-activated receptor family proteins (PPARs). Adipogenic stimuli induce the increased expression of PPARγ and C/EBPα. Subsequently, C/EBPα directly binds to PPARγ promoter and results in its expression. Previous studies have shown that Notch signaling is involved in adipogenesis, however, paradoxical results were observed with Notch signaling either promoting or inhibiting the differentiation of 3T3-L1 preadipocytes [8, 12]. In human primary cell cultures, inhibition of Notch signaling has been shown to facilitate adipogenic differentiation of adipose-derived mesenchymal stem cells [13].

Several strategies have been developed to target the Notch signaling pathway. They include antibodies that block Notch-1, −2, and −3 receptors, decoys that compete with the endogenous Notch receptors or ligands, peptides that interfere with the transcriptional complex formed by NICD, RBPJ and coactivators, as well as γ-secretase inhibitors (GSIs) that block the cleavage of NICD [14]. Over the past decades, GSIs have been extensively investigated for the potential to block the generation of amyloid β-peptide that is associated with neurodegeneration observed in Alzheimer's disease patients [15]. Two promising compounds are currently being evaluated in clinical trials for the treatment of Alzheimer's disease, including LY450139 (originally developed by Eli Lilly and Company, IN, USA; Phase 3) and BMS-708163 (originally developed by Bristol-Myers Squibb, NY, USA; Phase 2). Since Notch receptor cleavage and amyloid precursor protein processing are triggered by a similar proteolytic process mediated by γ-secretase, GSIs are also investigated at different stages of clinical trials for the treatment of neoplastic diseases and tumors known to harbor constitutive Notch activation. For instance, a phase 3 clinical trial for a GSI, PF-03084014 (developed by Pfizer, NY, USA), has been launched for determining its safety and efficacy in the treatment of desmoid tumor/aggressive fibromatosis [16].

Previous studies on the role of Notch signaling in adipogenesis has principally focused on white adipocyte differentiation with few studies reporting how Notch signaling regulates beige adipogenesis and mitochondrial biogenesis [17, 18]. In addition, although several GSIs, such as GSI-XI (N-[N-(3,5-Difluorophenacetyl)-l-alanyl]-S-phenylglycine t-butyl ester, DAPT) and dibenzazepine, have been used to inhibit Notch signaling, many of which are currently at the basic research or preclinical stage, limiting the translation of fundamental findings into clinical practice. Herein, we screened for the first time seven GSIs that have been investigated in clinical trials for the treatment of Alzheimer's disease or cancer. Their

efficiency in inhibition of Notch signaling and promotion of adipocyte browning as well as mitochondrial biogenesis was systematically compared using *in vitro* culture of 3T3-L1 pre-adipocytes. These findings provide insights into the effects of Notch inhibition in the metabolism of adipose tissue, highlight the potential of cross-therapeutic application of GSIs to obesity treatment via inhibition of γ-secretase mediated processing of Notch signaling, and bridge the gap between basic science and clinical investigation.

MATERIALS AND METHODS

Materials

MK-0752 was purchased from APExBIO (Houston, TX, USA). RO4929097, PF-03084014, LY3039478, and LY450139 were obtained from Selleckchem (Houston, TX, USA). BMS-708163 and BMS-906024 were purchased from Tocris Bioscience (Bristol, UK) and MilliporeSigma (Burlington, MA, USA), respectively. CellTiter 96® AQ$_{ueous}$ one solution reagent containing a tetrazolium compound [3-(4,5-dimethylthiazol-2-yl)-5-(3-carboxymethoxyphenyl)-2-(4-sulfophenyl)-2H-tetrazolium, inner salt; MTS] was purchased from Promega (Madison, WI, USA). Propidium iodide (P4864) was purchased from Sigma-Aldrich (St. Louis, MO, USA). UCP1 antibody (ab10983) and goat polyclonal secondary antibody to rabbit immunoglobulin G (IgG) - H&L (Alexa Fluor® 488, ab150077) were obtained from Abcam (Cambridge, UK). CCAAT/enhancer-binding protein alpha (C/EBPα, SC-61), and β-Actin (SC-47778) antibodies were purchased from Santa Cruz Biotechnology (Dallas, TX, USA). Cleaved caspase-3 (9661S), peroxisome proliferator-activated receptor gamma (PPARγ, 81B8), and horseradish peroxidase (HRP)-conjugated secondary antibodies, including anti-rabbit IgG (7074S) and anti-mouse IgG (7076S), were purchased from Cell Signaling Technology (Danvers, MA, USA). All other reagents and solvents were purchased from Sigma-Aldrich.

Cell Culture and Drug Treatment

3T3-L1 preadipocytes were cultured in Dulbecco's modified Eagle medium (DMEM) supplemented with 10% fetal bovine serum (FBS) and 1% antibiotics (penicillin and streptomycin) at 37°C, 5% CO$_2$, and 95% relative humidity. The medium was routinely changed every two days and cells were separated by trypsin before reaching confluency. Beige adipocyte differentiation was induced by treating confluent preadipocytes with the adipogenic induction medium containing DMEM, 10% FBS, 0.5 mM isobutylmethylxanthine, 1 μM dexamethasone, 1.75 μM insulin, and 1 μM rosiglitazone. Three days after induction, medium was switched to the differentiation medium containing DMEM, 10% FBS, 850 nM insulin, and 10 nM triiodothyronine until adipocytes matured. For the drug treatment, a series of GSIs were added to the cells in culture medium at the same final drug concentrations of 0.5, 1, and 10 μM, respectively, and cells were induced for differentiation.

Assessment of Cell Proliferation

Effects of GSIs at three concentrations on cell proliferation were determined using an MTS assay, which is based on the mitochondrial conversion of a tetrazolium salt. 3T3-L1 preadipocytes were seeded onto 96-well plates at a density of 1×10^4 cells per well and cultured in 5% CO$_2$ at 37°C for 48 h. GSIs were then added to the cells in culture medium at the same final drug concentrations of 0.5, 1, and 10 μM, respectively, and cells were further incubated at 37°C for 12 h. Subsequently, 20 μL of CellTiter 96® AQ$_{ueous}$ one solution reagent was added to each well in 100 μL of culture medium and incubated at 37°C in a humidified, 5% CO$_2$ atmosphere for 2 h. The absorbance was measured using a Tecan Spark™ 10 M microplate reader (Tecan, Männedorf, Switzerland) at a wavelength of 490 nm with background subtraction at 680 nm. Cells incubated with 0.1% Triton X-100 and dimethyl sulfoxide (DMSO) in culture medium served as positive and negative controls, respectively.

Cell Viability and Apoptosis Assays

3T3-L1 preadipocytes were treated with GSIs at a final drug concentration of 10 μM for 12 h at 37°C. After treatment, cells were stained with propidium iodide (1:500) and Hoechst 33342 (1:1000) in phosphate buffered saline (PBS) for 10 min at 37°C. Propidium iodide labeled cells were considered dead cells. For apoptosis analysis, the level of cleaved caspase-3 was used as a marker. Briefly, cells were fixed with 4% paraformaldehyde (PFA), quenched with glycine (100 mM glycine and 0.1% sodium azide in PBS), and blocked with PBS containing 2% BSA, 5% goat serum, and 0.2% Triton X-100 for 1 h at room temperature. Subsequently, cells were incubated with the cleaved caspase-3 antibody diluted at 1:300 in the same blocking buffer overnight at 4°C and the Alexa Fluor® 488 conjugated goat anti-rabbit IgG (1:1000 dilution) for 1 h at room temperature. Nuclei were counterstained with 4′,6-diamidino-2-phenylindole (DAPI, 1 μg/mL), which was pre-mixed with the secondary antibody. The stained cells were photographed using a CoolSnap HQ charge coupled-device camera installed on a Leica DMI 6000B microscope (Leica Camera, Wetzlar, Germany) with a × 20 objective.

Morphological Observation of Lipid Droplets

The morphology of mature adipocytes after treatments with various GSIs was observed using a Leica DMI 6000B microscope with a ×20 objective. Oil Red O staining was subsequently conducted to demonstrate the presence of accumulated lipid droplets in the cells. Briefly, cells were fixed with 4% PFA and stained with freshly prepared Oil Red O working solutions containing 6 mL of Oil Red O stock stain (5 mg/mL in isopropanol) and 4 mL of ddH_2O for 15 min. The stained cells were washed repeatedly with PBS and photographed using an OMAX 14 MP USB3.0 camera installed on a Leica DMI 6000B microscope with a ×20 objective. After imaging, Oil Red O was extracted from stained cells using isopropanol and absorbance was determined spectrophotometrically at a wavelength of 500 nm.

RNA Extraction, cDNA Synthesis, and Real-Time qPCR

Total RNA was extracted from cells using TRIzol (Thermo Fisher Scientific, Waltham, MA, USA) in accordance with the manufacturer's protocol. RNA was treated with RNase-free DNase I to remove contaminating genomic DNA and the purity as well as concentration of extracted RNA were determined by a spectrophotometer NanoDrop 2000c (Thermo Fisher Scientific, Waltham, MA, USA). Subsequently, 2 µg of RNA was reverse transcribed to cDNA using random hexamer primers with M-MLV reverse transcriptase (Invitrogen, Carlsbad, CA, USA). Real-time qPCR was performed in the Roche Light Cycler 480 PCR system (Roche, Basel, Switzerland) with SYBR Green master mix. The sequences of gene-specific primers were listed in Table S1. The $2^{-\Delta\Delta CT}$ method was used to analyze the relative changes of gene expression after normalization to the expression of *β-Actin*.

Protein Extraction and Western Blotting

Total protein was extracted from cells using RIPA buffer containing 25 mM Tris-HCl (pH 8.0), 150 mM NaCl, 1 mM EDTA, 0.5% NP-40, 0.5% sodium deoxycholate and 0.1% SDS. Protein concentrations were determined by Pierce BCA Protein Assay Reagent (Pierce Biotechnology, Waltham, MA, USA). Proteins were separated by SDS-PAGE and transferred to a polyvinylidene fluoride membrane (Millipore, Burlington, MA, USA). The membrane was then blocked with 5% fat-free milk for 1 h at room temperature and incubated with primary antibodies in 5% milk overnight at 4°C as well as secondary antibodies for 1 h at room temperature. Primary antibodies, including UCP1 (1:1000 dilution), C/EBPα (1:500 dilution), PPARγ (1:500 dilution), and β-Actin (1:5000 dilution), were used. HRP-conjugated secondary antibodies, including anti-rabbit

and anti-mouse IgG, were also used at a dilution of 1:10,000. A luminol reagent for enhanced chemiluminescence detection of western blots (Santa Cruz Biotechnology, Dallas, TX, USA) was employed and signals were detected with a FluorChem R imaging system (ProteinSimple, San Jose, CA, USA).

Immunofluorescence Staining of UCP1

Cells were fixed with 4% PFA, quenched with glycine, and blocked with PBS containing 2% BSA, 5% goat serum, and 0.2% Triton X-100 for 1 h at room temperature. Subsequently, cells were incubated with the UCP1 antibody diluted at 1:500 in the same blocking buffer overnight at 4°C and the Alexa Fluor® 488 conjugated goat anti-rabbit IgG (1:1000 dilution) for 1 h at room temperature. Nuclei were counterstained with DAPI (1 µg/mL), which was premixed with the secondary antibody.

Statistical Analysis

All studies were performed in triplicate and data points were expressed as mean values plus or minus standard error of the mean (mean ± SEM). To determine statistical significance, analysis of variance (one-way or two-way ANOVA) followed by Tukey's multiple comparison test was performed using GraphPad Prism 7. Differences were considered statistically significant if $p \le 0.05$.
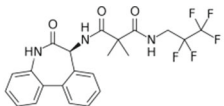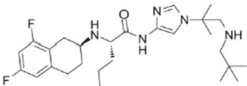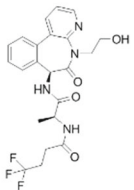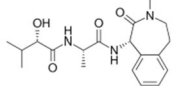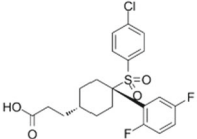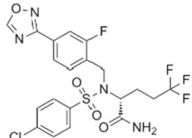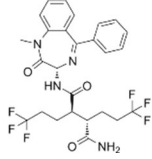
RESULTS

Effects of GSIs on Notch Inhibition

To determine the impact of GSIs on inhibition of Notch signaling, 3T3-L1 preadipocytes were treated with a series of GSIs (Table 1) at a concentration of 1 µM and the change in mRNA level of *Hes1*, a Notch downstream transcriptional target gene, was evaluated using real-time qPCR. As shown in Fig. 1A, the expression of *Hes1* was significantly inhibited after the treatment with RO4929097 ($p \le 0.01$), PF-03084014 ($p \le 0.01$), LY3039478 ($p \le 0.001$), and BMS-906024 ($p \le 0.001$), suggesting efficient inhibition of Notch signaling. However, other GSIs used in the experiment, including LY450139, MK-0752, and BMS-708163, did not significantly decrease the expression level of *Hes1* at the concentration of 1 µM (Fig. 1A). The difference in inhibitory activity of Notch signaling among drug treatments might be due to variable effective concentrations.

To further examine the relationship between drug concentration and inhibitory effect of GSIs, cells were

Table I   Seven GSIs used in this study

Compound	Chemical structure	Originally developed by	Study phase	Condition or disease
RO4929097		Roche	2	Metastatic colorectal cancer; recurrent or progressive glioblastoma; renal cell carcinoma; metastatic pancreas cancer; recurrent and/or metastatic epithelial ovarian cancer, fallopian tube cancer, or primary peritoneal cancer
PF-03084014		Pfizer	3	Desmoid tumor/aggressive fibromatosis
LY3039478		Eli Lilly	2	T-cell acute lymphoblastic leukemia; T-cell lymphoblastic lymphoma
LY450139		Eli Lilly	3	Alzheimer's disease
MK-0752		Merck	2	Metastatic breast cancer
BMS-708163		Bristol-Myers Squibb	2	Alzheimer's disease
BMS-906024		Bristol-Myers Squibb	2	Adenoid cystic carcinoma

treated with the four most promising inhibitors (i.e. RO4929097, PF-03084014, LY3039478, and BMS-906024) at three gradient concentrations (0.5, 1, and 10 μM). It was observed that the mRNA level of *Hes1* was significantly downregulated by 40–50% across all the treatment groups compared to the DMSO control group ($p \leq 0.01$), even at the lowest concentration of 0.5 μM (Fig. 1B). The inhibitory effects became stronger with increasing concentrations of PF-03084014, LY3039478, and BMS-906024, whereas the treatment of RO4929097 did not result in a dose-dependent depression in *Hes1* expression. These results suggest that 3T3-L1 preadipocytes respond to a variety of GSIs with different sensitivity.
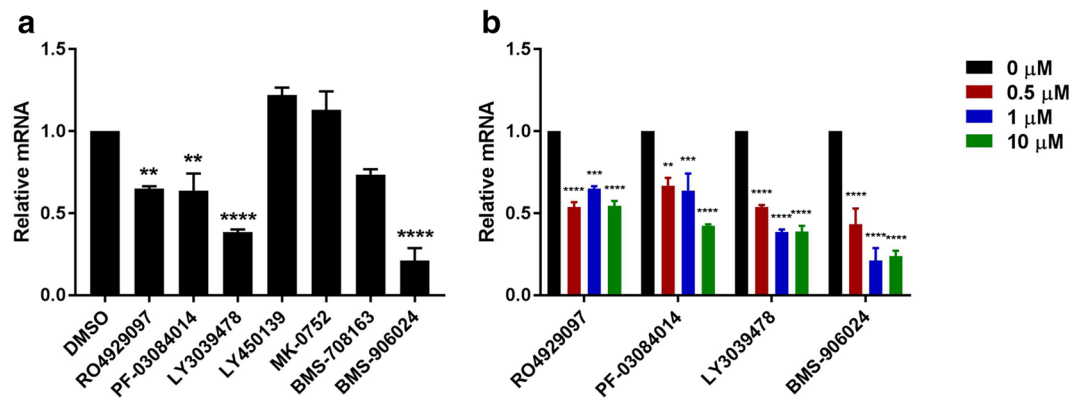
Fig. 1 Effects of GSIs on Notch inhibition. (**a**) Real-time qPCR analysis showing the mRNA levels of the Notch target gene *Hes1* in 3T3-L1 preadipocytes after 12 h treatments with seven GSIs at a concentration of 1 μM; (**b**) Real-time qPCR analysis showing the mRNA levels of *Hes1* in 3T3-L1 preadipocytes after 12 h treatments with four most efficient GSIs at concentrations of 0, 0.5, 1, and 10 μM. $^*p < 0.05$, $^{**}p < 0.01$, $^{***}p < 0.005$ and $^{****}p < 0.001$ (One-way or two-way ANOVA followed by Tukey's multiple comparison test). Data are shown as mean ± SEM. $n = 3$ individual experiments
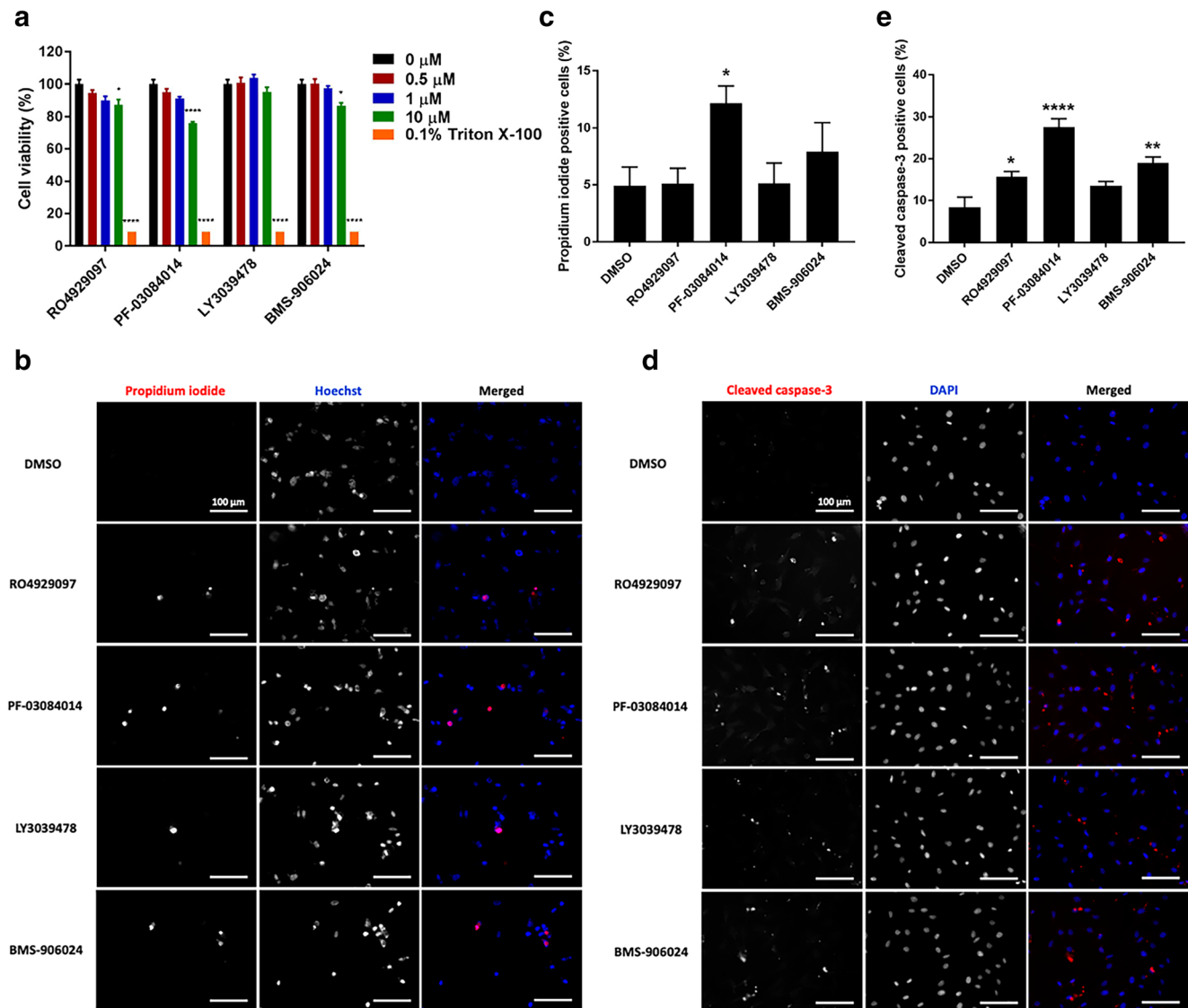
Effects of GSIs on Cell Proliferation and Viability

To investigate the cytotoxicity of GSIs in 3T3-L1 preadipocytes, cells were treated with GSIs at three gradient concentrations (0.5, 1, and 10 μM) for 12 h and cell proliferation was measured by an MTS assay. It was found that RO4929097, PF-03084014, and BMS-906024 inhibited cell proliferation (Fig. 2A). Induction of cytotoxicity by these three GSIs was dose-dependent with most considerable effects observed at the highest concentration of 10 μM, particularly in the group treated with PF-03084014 ($p \leq 0.001$). The result is consistent with previously published data, showing inhibition of cell growth by PF-03084014 might be partially due to its effect on induction of cell cycle block and apoptosis [19]. To further address whether high-dose GSIs-induced cytotoxicity is mediated through apoptotic cell death, 3T3-L1 preadipocytes were incubated GSIs at 10 μM for 12 h and stained with propidium iodide. As shown in Fig. 2B and C, the percent propidium iodide positive cells increased in the GSI-treated groups compared to that in the vehicle control group. The difference was statistically significant between PF-03084014 and DMSO treated cells ($p \leq 0.05$), suggesting that cells were undergoing cell death. To better understand if GSI-induced cell death is due to apoptosis, the level of activated caspase-3 was determined through staining the cleaved substrate. Compared to the control group, the percent caspase-3 positive cells significantly increased in GSI-treated groups, including RO4929097 ($p \leq 0.05$), PF-03084014 ($p \leq 0.001$), and BMS-906024 ($p \leq 0.01$) (Fig. 2D and E). This confirmed the involvement of caspase-3 in high-dose GSI-induced apoptosis, although additional caspase-independent mechanisms could also contribute to the cell death. It was noted that the treatment with LY3039478 even at the highest concentration of 10 μM did not result in any significant changes in cell proliferation and viability, indicating the promising safety of this compound.

GSIs Promote Differentiation Efficiency of 3T3-L1 Preadipocytes

To determine the role of Notch signaling in adipogenesis, 3T3-L1 preadipocytes were treated with various GSIs at three gradient concentrations (0.5, 1, and 10 μM) after induced to differentiate. As shown in Fig. 3A, differentiation of 3T3-L1 cells was efficiently induced with lipid droplets accumulated in the cytoplasm after incubation with induction medium for three days followed by differentiation medium for five days. Both phase contrast and Oil Red O staining images confirmed that the number and size of lipid droplets increased in the GSI (1 μM) treated cells compared to the DMSO control, suggesting that GSIs enhanced the differentiation efficiency of 3T3-L1 cells. However, no obvious differences were observed among the four compounds. It was also noted that three gradient concentrations did not cause remarkable differences in the number and size of lipid droplets (Fig. S1). Total lipid content within the cells was further determined by quantitative analysis of Oil Red O intensity. Results show that the absorbance value of Oil Red O extracted from the GSI treated cells was significantly higher than that in the control group (Fig. 3B), demonstrating that even very low dosages of GSIs promote the differentiation of 3T3-L1 cells and accumulation of lipid droplets.

GSIs Upregulate the Expression of Beige Adipogenic and Browning Marker Genes in Differentiated 3T3-L1 Cells

Although the Notch signaling has been shown to affect adipocyte differentiation, its potential role in regulation of beige adipocyte biogenesis has only been investigated recently [17]. To identify the impact of GSIs on beige adipogenesis,

Fig. 2 Effects of GSIs on cell proliferation and viability. (**a**) MTS assay showing dose-dependent cytotoxicity and inhibitory effects of cell proliferation induced by GSIs at concentrations of 0.5, 1, and 10 μM after 12 h of incubation. DMSO negative control without any inhibitors (0 μM) and 0.1% Triton X-100 positive control were included; (**b**) Propidium iodide staining showing an increase in cell death when treating 3T3-L1 preadipocytes with GSIs at a high concentration (10 μM); (**c**) Quantification of percent propidium iodide positive cells; (**d**) Induction of apoptotic cell death was accompanied by cleavage of caspase-3 as demonstrated by immunofluorescence staining; (**e**) Quantification of percent cleaved caspase-3 positive cells. $^{*}p < 0.05$, $^{**}p < 0.01$, $^{***}p < 0.005$ and $^{****}p < 0.001$ (One-way or two-way ANOVA followed by Tukey's multiple comparison test). Data are shown as mean ± SEM. $n = 3$ individual experiments

we examined the mRNA expression of adipogenic, mitochondria-related, and beige fat-selective genes in differentiated 3T3-L1 cells following the consecutive treatment with GSIs using real-time qPCR. As shown in Fig. 4A, the expression of fatty acid binding protein 4 (*Fabp4*) increased in the cells treated with GSIs at all the concentrations; however, the differences were not significant. The GSI treatments also upregulated the expression of peroxisome proliferator-activated receptor gamma coactivator 1-alpha (*Ppargc1α*) with significant changes observed in the groups treated with PF-03084014 and LY3039478 at the highest concentration of 10 μM ($p ≤ 0.05$). In addition, Fig. 4B shows that RO4929097 increased

the expression of cytochrome c oxidase subunit 5B (*Cox5B*) at all the concentrations with the low dose treatment inducing the most significant change ($p ≤ 0.001$). Significant upregulation of *Cox5B* was also observed when cells were treated with 1 μM of PF-03084014 ($p ≤ 0.01$) and 10 μM of LY3039478 ($p ≤ 0.05$). PF-03084014, LY3039478, and BMS-906024 increased the expression of transmembrane protein 26 (*Tmem26*) in a dose-dependent manner with the highest dose causing significant differences between treatment and control groups. Furthermore, the expression of beige fat-selective genes, including uncoupling protein 1 (*Ucp1*), cell death-inducing DNA fragmentation factor alpha-
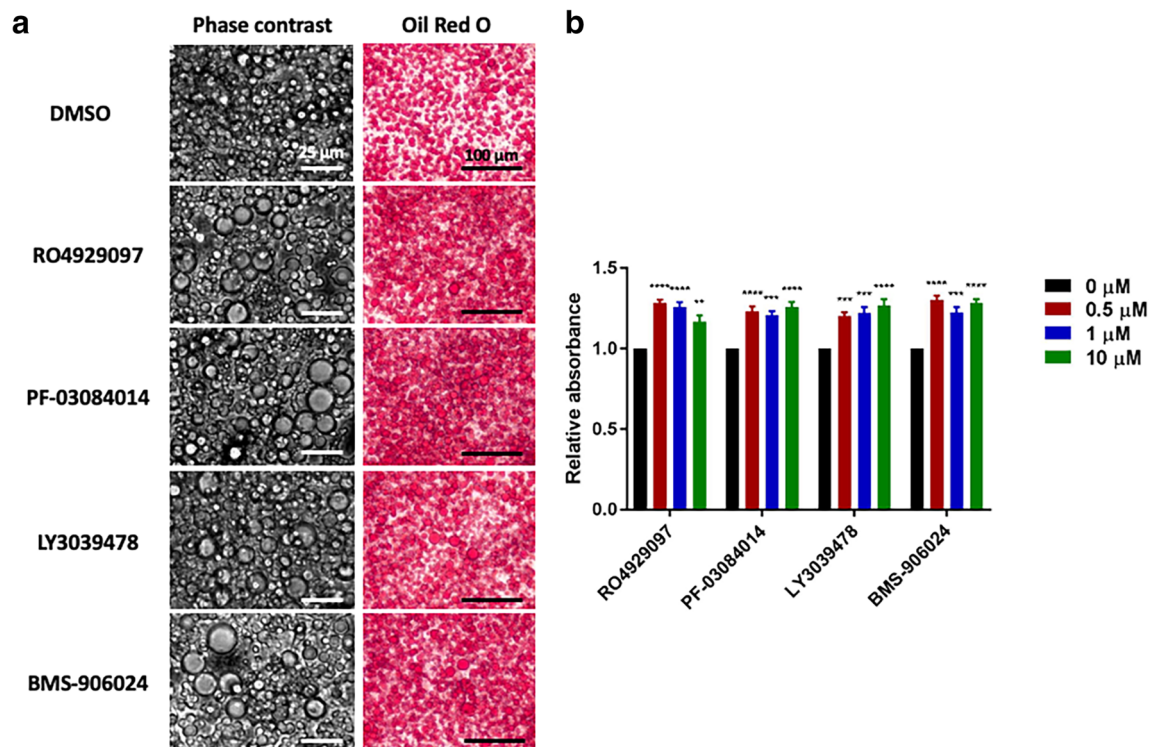
Fig. 3 GSIs promote differentiation efficiency of 3T3-L1 preadipocytes. 3T3-L1 preadipocytes were treated with four GSIs at concentrations of 0.5, 1, and 10 μM and induced for differentiation. A DMSO vehicle control without any inhibitors (0 μM) was also included. Medium containing GSIs were routinely changed every two days during differentiation. (**a**) Representative phase contrast and bright field images of differentiated 3T3-L1 cells stained with Oil Red O after the treatment with GSIs at the concentration of 1 μM; (**b**) Relative absorbance at 500 nm of cell lysates extracted from Oil Red O stained cells treated with different concentrations of GSIs. $^{*}p < 0.05$, $^{**}p < 0.01$, $^{***}p < 0.005$ and $^{****}p < 0.001$ (Two-way ANOVA followed by Tukey's multiple comparison test). Data are shown as mean $\pm$ SEM. n = 3 individual experiments

like effector A (*Cidea*), PR domain containing 16 (*Prdm16*), and type 2 deiodinase (*Dio2*), was upregulated after the treatment with all the GSIs (Fig. 4C). However, significant changes were found only in the groups of PF-03084014 and LY3039478 with the high concentration of 10 μM ($p \leq 0.05$). These results indicate that GSIs promote beige adipogenesis and mitochondrial biogenesis in differentiated adipocytes, but the optimal concentrations to achieve the maximum efficiency are variable for each compound.

Western blot analysis revealed that the protein expression of UCP1 was significantly upregulated when cells were treated with 1 μM of RO4929097 ($p \leq 0.05$) and PF-03084014 ($p \leq 0.01$) (Fig. 4D and E). However, the enhancement in expression level was decreased by approximately 50% when the concentration of GSIs increased from 1 μM to 10 μM, which might be attributed to the cytotoxicity induced by the high dose. The protein levels of adipogenic markers, such as PPARγ and C/EBPα, were also evaluated (Fig. 4D and E). It was found that four GSIs significantly increased the expression level of PPARγ at all concentrations examined. The expression of C/EBPα was significantly upregulated

after the treatment with RO4929097 and LY3039478 at all the concentrations as well as 1 μM of BMS-906024 ($p \leq 0.005$). These results suggest that Notch inhibition mediated by GSIs promote adipogenesis and browning of white adipocytes. It was also noted that the low concentration of 0.5 μM was sufficient to increase the protein expression of PPARγ, but a higher concentration of 1 μM was required to induce significant upregulation of UCP1.

GSIs Promote the Protein Expression of UCP1 in Differentiated 3T3-L1 Cells

To further confirm whether GSI enhances thermogenic activities of UCP1 at the cellular level, the expression of UCP1 in 3T3-L1 cells after the treatment with GSIs at the concentration of 1 μM was investigated by immunofluorescence staining. As shown in Fig. 5, the green fluorescence signal indicating UCP1 positive staining was detected in the cytoplasm of 3T3-L1 cells. Only few UCP1 positive adipocytes were observed in the DMSO control group, while a number of adipocytes expressing UCP1 were seen in GSI treated groups. Compared to RO4929097, PF-03084014, and LY3039478,
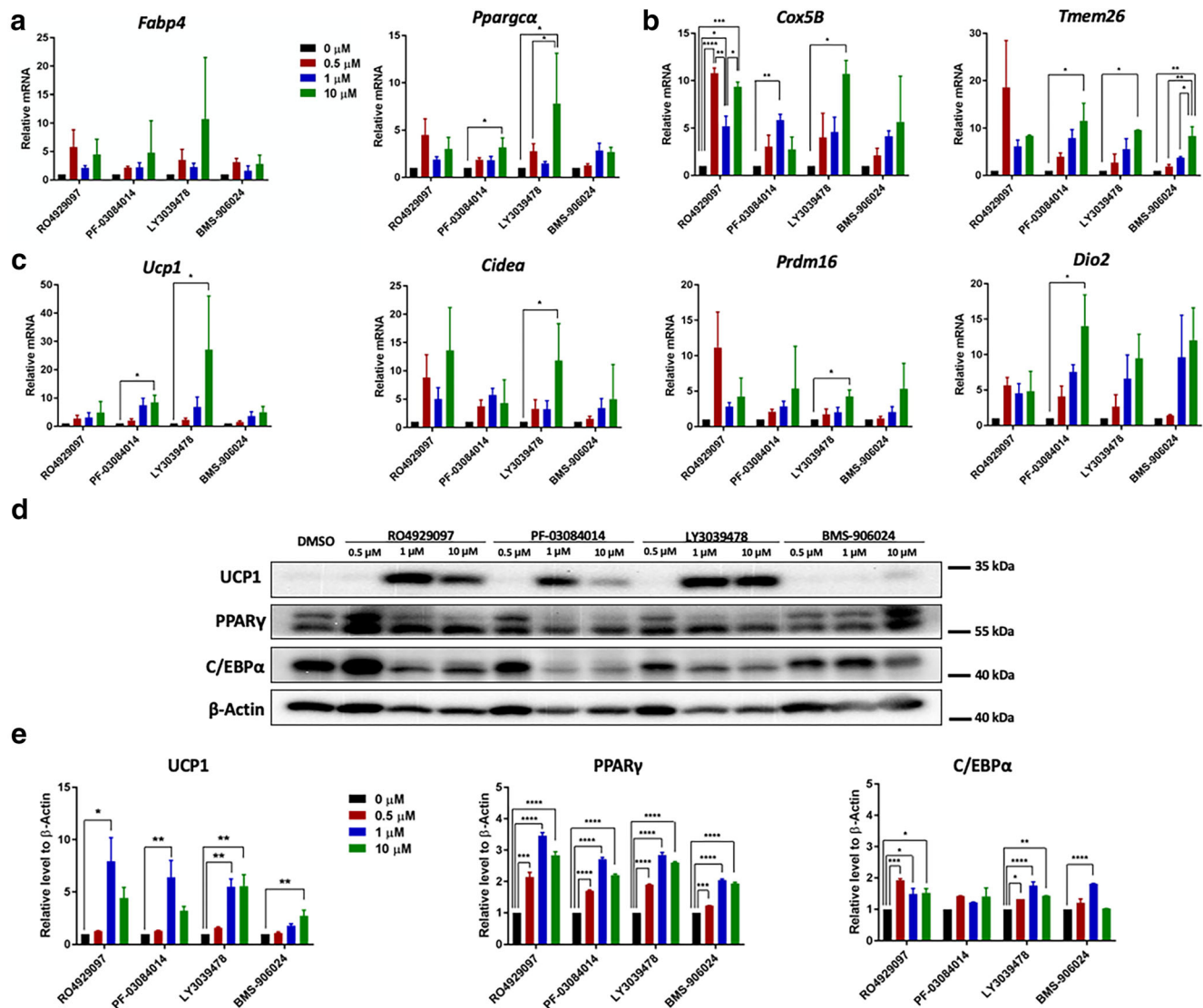
Fig. 4 GSIs upregulate the expression of beige adipogenic and browning marker genes in differentiated 3T3-L1 cells. (A-C) Real-time qPCR analysis showing the relative mRNA levels of adipogenic genes, including *Fabp4* and *Ppargcα* (**a**), mitochondrial and beige cell surface marker genes, including *Cox5B* and *Tmem26* (**b**), and browning marker genes, including *Ucp1*, *Cidea*, *Prdm16*, and *Dio2* (**c**); (**d**) Western blot results showing relative protein abundance of UCP1, PPARγ, and C/EBPα in differentiated 3T3-L1 cells treated with GSIs at three concentrations; (**e**) Quantification of the relative protein levels of UCP1, PPARγ, and C/EBPα normalized to β-Actin controls by densitometry analysis. $^*p < 0.05$, $^{**}p < 0.01$, $^{***}p < 0.005$ and $^{****}p < 0.001$ (Two-way ANOVA followed by Tukey's multiple comparison test). Data are shown as mean ± SEM. n = 3 individual experiments

BMS-906024 at the same concentration showed the minimal efficiency in increasing UCP1 expression, which is consistent with western blot results shown in Fig. 4D and E. Taken together, our results demonstrate that GSIs could induce browning of white adipocytes by upregulating UCP1 expression.

DISCUSSION

Notch signaling, an evolutionarily highly conserved pathway, is important in regulating cell-cell communication and cell-fate determination during normal development of most organs and tissues in the body. It has also been reported that Notch signaling is required in tissue homeostasis, such as hematopoietic system [20], vasculature [21], skeletal muscle [22], and adipose tissue [17]. Although understanding of signaling pathways that regulate adipogenesis has been considered a fundamental for the treatment of obesity with the role of Notch signaling characterized by various research groups [23, 24], its function in modulating the adipocyte plasticity and beige adipocyte biogenesis has just been discovered recently [17]. Our group has previously found that Notch signaling plays an important role in regulating adipocyte
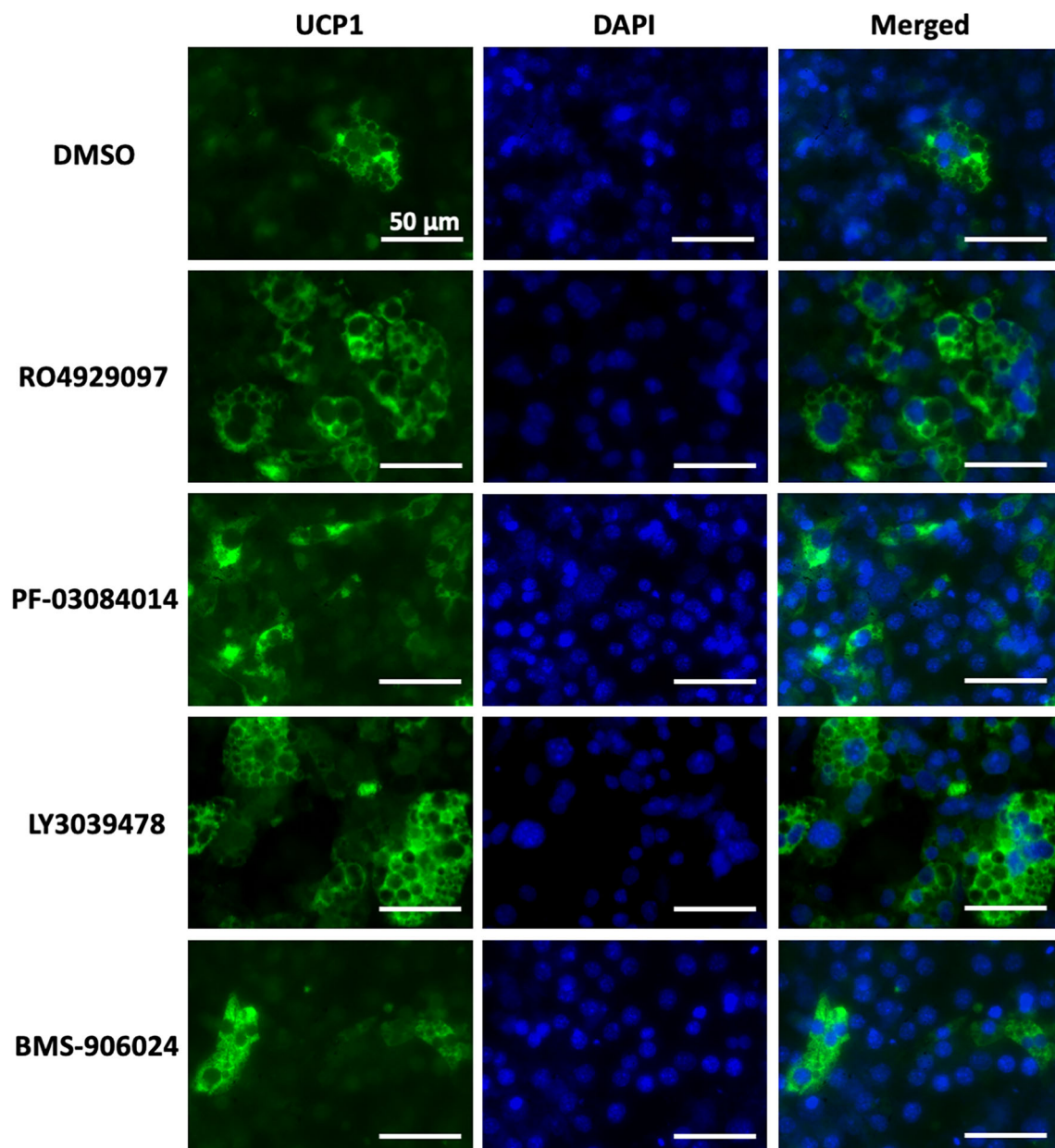
Fig. 5 GSIs increase the protein expression of UCP1 in differentiated 3T3-L1 cells. 3T3-L1 preadipocytes were treated with four GSIs at the concentrations of 1 μM and induced for differentiation. A DMSO vehicle control without any inhibitors (0 μM) was also included. Medium containing GSIs were routinely changed every two days during differentiation. UCP1 was stained with Alexa Fluor® 488 in green and nuclei were counterstained with DAPI in blue

thermogenesis as well as conversion of white to beige adipocytes in mice, consequently affecting body energy metabolism [17]. It has been demonstrated that pharmacological inhibition of Notch signaling through administration of dibenzazepine promotes widespread browning of WAT. Specifically, the browning phenotype leads to metabolic beneficial effects, including enhanced energy expenditure, glucose tolerance, insulin sensitivity, and resistance to high fat diet-induced obesity. However, dibenzazepine is currently used for research only and its effects in humans have not been studied, challenging the translation of fundamental findings into clinical

practice. Here, we screened a series of GSIs that have been found to be reasonably safe in phase 1 clinical trials and are currently being investigated in phase 2 or 3 for the treatment of cancer or Alzheimer's disease. Their impacts on inhibition of Notch signaling pathway and induction of browning of white adipocytes were systematically compared.

We found that four of seven GSIs, including RO4929097, PF-03084014, LY3039478, and BMS-906024, at the concentration of 1 μM significantly downregulated the mRNA expression of Notch downstream target gene *Hes1* in the initial screening. The differences in inhibitory activity of Notch

signaling induced by GSIs might be attributed to variable isoform-specific binding sites and mechanisms of action. In general, selective isoform inhibition is considered a relatively safe therapeutic strategy with reduced systemic toxicity, pan-inhibitors, on the other hand, could display enhanced inhibitory efficiency [25]. Indeed, our present results showed that isoform-specific inhibitors, such as BMS-708163 and MK-0752, exhibited relatively moderate inhibitory effect of Notch signaling compared to other pan-Notch inhibitors. However, which class of agents between isoform-specific or pan-inhibitors can achieve better treatment results is still an open question and further investigations associated with toxicology profile and clinical efficacy are certainly required. Another possible factor that may contribute to the differences among these GSIs is the selectivity of blocking target. For instance, a GSI compound might not be specific for γ-secretase cleavage of Notch receptors, and can also inhibit the processing of many other γ-secretase substrates, such as β-amyloid. The comprehensive blocking mechanisms could lead to distinct pharmacological consequences. The selected four compounds at three gradient concentrations were further investigated in the secondary screening with efficient inhibition of Notch achieved even at the lowest concentration of 0.5 μM. PF-03084014, LY3039478, and BMS-906024 exhibited a dose-dependent inhibition of Notch, whereas RO4929097 did not display a clear correlation between drug concentration and inhibitory activity in the range between 0.5 to 10 μM. This result suggests RO4929097 could be a very potent GSI targeting Notch signaling and the inhibitory activity might have reached its threshold at the concentration of 0.5 μM. Previously, *in vitro* inhibitory activity of Notch induced by RO4929097 has also been evaluated in human tumor-derived cells by Roche [26]. They found that the compound treatment led to a dose-dependent inhibition beginning at 0.1 μM, but no further reduction in protein and mRNA levels of *Hes1* was observed when the concentration was higher than 0.5 and 1 μM, respectively.

We next determined the cytotoxicity of GSIs at three concentrations in 3T3-L1 preadipocytes. We found that inhibiting γ-secretase activity by LY3039478 had no significant effects on cell proliferation and viability at all the concentrations used. In contrast, RO4929097, PF-03084014, and BMS-906024 inhibited cell growth in a dose-dependent manner and the reduction in cell viability was more considerable at high doses. The cytotoxic effect of high-dose GSIs resulted from induction of apoptotic cell death, which was also accompanied by increased cleaved levels of caspase-3. Previous studies have shown inhibition of Notch pathway can induce cell apoptosis and cell cycle arrest through regulating the expressions of apoptotic factors and cell cycle proteins [27, 28]. However, whether the cytotoxicity of GSIs is mediated by inhibition of proteasome activity or γ-secretase mediated processing of Notch signaling has also been a subject of ongoing

investigation. For instance, Han et al. determined the cytotoxicity of GSI I in a number of cell lines, but the treatment with two highly specific GSI did not affect the survival of these cells [29]. The authors concluded that inhibition of proteasome activity was the major contributor to the observed cytotoxicity. Nevertheless, several questions regarding the action of GSIs in Notch signaling-independent mechanisms remain to be answered. Furthermore, in order to achieve enhanced intracellular transport of GSIs with minimized cytotoxicity, development of clinically translatable Notch-inhibiting drug delivery systems could be one of our future directions [18, 30].

More importantly, we found that the treatment with GSIs promoted differentiation of 3T3-L1 preadipocytes and upregulated adipogenic marker genes at the level of transcription and translation. Our results are supported by previously reported data, showing that the Notch signaling is a negative regulator in adipogenesis of 3T3-L1 preadipocytes [31]. The process of adipogenesis involves downregulation of the gene encoding *Hes1*, which plays a dual role in adipocyte development as a suppresser and an activator. However, promoter analyses of up- and down-regulated genes in 3T3-L1 preadipocytes has demonstrated that the Notch signaling most likely inhibits adipogenesis through induction of *Hes1* homodimers, which block the transcription of target genes. In addition, this effect could also be achieved by exposing 3T3-L1 preadipocytes to the Notch ligand Jagged1, associating with complete loss of PPARγ and C/EBPα [32]. This is supported by the findings in our study that GSIs, even at the lowest concentration of 0.5 μM, are effective to induce the depressed transcription of *Hes1* and the increased expression of adipogenic marker genes. Although PPARγ and C/EBPα are important regulators of the thermogenic program of beige adipocytes, additional transcriptional components that cooperate with them, particularly PRDM16 and PGCα, have been shown to be necessary to activate the beige fat-selective gene program [33, 34]. We therefore examined the expression of mitochondria-related and beige fat-selective genes. Results reveal that Notch inhibition induced by GSIs upregulate their expression levels, which is consistent with our previous findings [17].

Furthermore, we determined the expression of UCP1, which has long been considered the key protein stimulating thermogenesis by uncoupling cellular respiration and mitochondrial ATP synthesis as well as playing a crucial role in regulation of adipose conversion [35, 36]. In our study, significant upregulation of UCP1 was observed when cells were with RO4929097, PF-03084014, and LY3039478 at the concentration of 1 μM. Compared to these three compounds, BMS-906024 had the minimal impact on the increase in UCP1 protein expression. Interestingly, the upregulated expression of UCP1 decreased by around 50% when a higher concentration of 10 μM was used in the groups treated with RO4929097 and PF-03084014. In contrast, the high concentration of LY3039478, has shown to be less cytotoxic than

other compounds, did not significantly change the protein expression of UCP1. These results demonstrate that the efficiency of beige adipogenesis and browning of white adipocytes might be affected by the cytotoxicity induced by high-dose GSIs. Most studies to date use GSIs at a concentration of 10 μM to induce adipogenesis *in vitro* and investigate the role of Notch signaling [17, 37]; however, our present findings confirm the efficiency of potent GSIs with relatively low concentrations and point out the importance of selecting the optimal dose that is sufficient to achieve pharmacological activity and would be expected to alleviate toxicities associated with overdose.

A limitation of our present study is that we only focused on the canonical Notch target *Hes1*. Our previous studies have shown that *Hes1* directly binds to the promoter regions of *Prdm16* and *Ppargc1a* to inhibit the transcription of these two master regulators of mitochondrial biogenesis and beige adipogenesis [17]. However, other canonical and non-canonical Notch targets involved in adipogenesis and mitochondrial biogenesis could also be impacted by GSIs and contribute to the pleiotropic effects of Notch signaling. It is worth noting that non-canonical Notch signaling is RBPJ-independent and can be either ligand-dependent or independent [38]. The functions have mostly been identified in stem cells and progenitor cells which are capable of expansion and/or differentiation, suggesting that non-canonical signals might play a role in early cell populations and interact with conserved cell regulators [39]. The most well-studied and conserved effect of non-canonical Notch function is regulation of Wnt/β-catenin signaling [40]. Although canonical Notch signals are responsible for the majority of Notch signaling, further investigation of non-canonical Notch signaling modulated by GSIs is required to better predict the final pharmacological consequences of Notch targeting.

CONCLUSIONS

In the present study, we have shown that pharmacological inhibition of Notch signaling by clinical candidates of GSIs with an optimized concentration promotes beige adipogenesis and mitochondrial biogenesis in 3T3-L1 preadipocytes. These findings not only highlight the potential of cross-therapeutic application of GSIs to obesity treatment via inhibition of γ-secretase-mediated processing of Notch signaling, but also provide important experimental evidence to support further design and development of clinically translatable Notch-inhibiting drug delivery systems.

ACKNOWLEDGEMENTS

AUTHOR CONTRIBUTIONS

All authors contributed to the study conception and design. Material preparation, data collection, and analysis were performed by D. H. and J. Q. The manuscript was drafted by D. H. and revised by M. D. and S. K. All authors read and approved the final manuscript.

COMPLIANCE WITH ETHICAL STANDARDS

Declaration of Interests   M. D., D. H., and S. K. have applied for patents related to this study. M. D. is founder of Adipo Therapeutics, a university startup developing polymer technologies for applications in adipocytes.

REFERENCES

1. Smith KB, Smith MS. Obesity statistics. Prim care - Clin off Pract. Elsevier. 2016;43:121–35.

2. Huang D, Deng M, Kuang S. Polymeric carriers for controlled drug delivery in obesity treatment. Trends Endocrinol Metab Elsevier. 2019;30:974–89.

3. Rosen ED, Spiegelman BM. Adipocytes as regulators of energy balance and glucose homeostasis. Nature Nature Publishing Group. 2006;444:847–53.

4. Lshibashi J, Seale P. Beige can be slimming. Science (80-). American Association for the Advancement of Science. 2010;328: 1113–4.

5. Wu J, Boström P, Sparks LM, Ye L, Choi JH, Giang AH, et al. Beige adipocytes are a distinct type of thermogenic fat cell in mouse and human. Cell Elsevier. 2012;150:366–76.

6. Artavanis-Tsakonas S, Rand MD, Lake RJ. Notch signaling: cell fate control and signal integration in development. Science (80-). American Association for the Advancement of Science. 1999;284: 770–6.

7. Luo D, Renault VM, Rando TA. The regulation of notch signaling in muscle stem cell activation and postnatal myogenesis. Semin Cell Dev Biol Elsevier. 2005;16:612–22.

8. Urs S, Turner B, Tang Y, Rostama B, Small D, Liaw L. Effect of soluble Jagged1-mediated inhibition of notch signaling on proliferation and differentiation of an adipocyte progenitor cell model. Adipocyte Taylor & Francis. 2012;1:46–57.

9. Kadesch T. Notch signaling: the demise of elegant simplicity. Curr Opin Genet Dev Elsevier. 2004;14:506–12.

10. Schroeter EH, Kisslinger JA, Kopan R. Notch-1 signalling requires ligand-induced proteolytic release of intracellular domain. Nature. Nature Publishing Group. 1998;393:382–6.

11. Gregoire FM, Smas CM, Sul HS. Understanding adipocyte differentiation. Physiol rev. American Physiological Society Bethesda. MD. 1998;78:783–809.

12. Lai PY, Tsai C Bin, Tseng MJ. Active form Notch4 promotes the proliferation and differentiation of 3T3-L1 preadipocytes. Biochem Biophys res Commun. Elsevier; 2013;430:1132–9.

13. Osathanon T, Subbalekha K, Sastravaha P, Pavasant P. Notch signalling inhibits the adipogenic differentiation of single-cell-

derived mesenchymal stem cell clones isolated from human adipose tissue. Cell Biol Int Wiley Online Library. 2012;36:1161–70.

14. Espinoza I, Miele L. Notch inhibitors for cancer treatment. Pharmacol Ther Elsevier. 2013;139:95–110.

15. Woo HN, Park JS, Gwon AR, Arumugam TV, Jo DG. Alzheimer's disease and notch signaling. Biochem Biophys res Commun. Elsevier. 2009;390:1093–7.

16. SpringWorks Therapeutics. No Title [Internet]. 2020. Available from: clinicaltrials.gov/ct2/show/NCT03785964

17. Bi P, Shan T, Liu W, Yue F, Yang X, Liang XR, et al. Inhibition of notch signaling promotes browning of white adipose tissue and ameliorates obesity. Nat Med. 2014;20:911–8.

18. Jiang C, Cano-Vega MA, Yue F, Kuang L, Narayanan N, Uzunalli G, et al. Dibenzazepine-Loaded Nanoparticles Induce Local Browning of White Adipose Tissue to Counteract Obesity. Mol Ther. Elsevier Ltd. 2017;25:1718–29.

19. Wei P, Walls M, Qiu M, Ding R, Denlinger RH, Wong A, et al. Evaluation of selective γ-secretase inhibitor PF-03084014 for its antitumor efficacy and gastrointestinal safety to guide optimal clinical trial design. Mol Cancer Ther AACR. 2010;9:1618–28.

20. Kelly A, Houston SA, Sherwood E, Casulli J, Travis MA. Regulation of innate and adaptive immunity by TGFβ. Adv Immunol Nature Publishing Group. 2017;134:137–233.

21. Gridley T. Notch signaling in the vasculature. Curr Top Dev Biol. Elsevier; 2010. p. 277–309.

22. Mourikis P, Sambasivan R, Castel D, Rocheteau P, Bizzarro V, Tajbakhsh S. A critical requirement for notch signaling in maintenance of the quiescent skeletal muscle stem cell state. Stem Cells Wiley Online Library. 2012;30:243–52.

23. Garcés C, Ruiz-Hidalgo MJ, De Mora JF, Park C, Miele L, Goldstein J, et al. Notch-1 controls the expression of fatty acid-activated transcription factors and is required for adipogenesis. J Biol Chem ASBMB. 1997;272:29729–34.

24. Song BQ, Chi Y, Li X, Du WJ, Han ZB, Tian JJ, et al. Inhibition of notch signaling promotes the Adipogenic differentiation of Mesenchymal stem cells through autophagy activation and PTEN-PI3K/AKT/mTOR pathway. Cell Physiol Biochem Karger Publishers. 2015;36:1991–2002.

25. Lonetti A, Cappellini A, Spartà AM, Chiarini F, Buontempo F, Evangelisti C, et al. PI3K pan-inhibition impairs more efficiently proliferation and survival of T-cell acute lymphoblastic leukemia cell lines when compared to isoform-selective PI3K inhibitors. Oncotarget. Impact Journals, LLC; 2015;6:10399.

26. Luistro L, He W, Smith M, Packman K, Vilenchik M, Carvajal D, et al. Preclinical profile of a potent γ-secretase inhibitor targeting notch signaling with in vivo efficacy and pharmacodynamic properties. Cancer Res AACR. 2009;69:7672–80.

27. Kim SJ, Lee HW, Baek JH, Cho YH, Kang HG, Jeong JS, et al. Activation of nuclear PTEN by inhibition of notch signaling induces G2/M cell cycle arrest in gastric cancer. Oncogene Nature Publishing Group. 2016;35:251–60.

28. Sha J, Li J, Wang W, Pan L, Cheng J, Li L, et al. Curcumin induces G0/G1 arrest and apoptosis in hormone independent prostate cancer DU-145 cells by down regulating notch signaling. Biomed Pharmacother Elsevier. 2016;84:177–84.

29. Han J, Ma I, Hendzel MJ, Allalunis-Turner J. The cytotoxicity of γ-secretase inhibitor I to breast cancer cells is mediated by proteasome inhibition, not by γ-secretase inhibition. Breast Cancer Res. Springer; 2009;11:R57.

30. Huang D, Narayanan N, Cano-Vega MA, Jia Z, Ajuwon KM, Kuang S, et al. Nanoparticle-Mediated Inhibition of Notch Signaling Promotes Mitochondrial Biogenesis and Reduces Subcutaneous Adipose Tissue Expansion in Pigs. iScience. Elsevier; 2020;23:101167.

31. Ross DA, Rao PK, Kadesch T. Dual roles for the notch target gene Hes-1 in the differentiation of 3T3-L1 Preadipocytes. Mol Cell Biol Am Soc Microbiol. 2004;24:3505–13.

32. Ross DA, Hannenhalli S, Tobias JW, Cooch N, Shiekhattar R, Kadesch T. Functional analysis of Hes-1 in preadipocytes. Mol Endocrinol Oxford University Press. 2006;20:698–705.

33. Kajimura S, Seale P, Spiegelman BM. Transcriptional control of brown fat development. Cell Metab Elsevier. 2010;11:257–62.

34. Shapira SN, Seale P. Transcriptional control of Brown and Beige fat development and function. Obesity Elsevier. 2019;27:13–21.

35. Nedergaard J, Golozoubova V, Matthias A, Asadi A, Jacobsson A, Cannon B. UCP1: the only protein able to mediate adaptive non-shivering thermogenesis and metabolic inefficiency. Biochim Biophys Acta - Bioenerg. Elsevier. 2001;1504:82–106.

36. Shabalina IG, Petrovic N, deJong JMA, Kalinovich A V., Cannon B, Nedergaard J. UCP1 in Brite/beige adipose tissue mitochondria is functionally thermogenic. Cell rep. Elsevier; 2013;5:1196–203.

37. Huang Y, Yang X, Wu Y, Jing W, Cai X, Tang W, et al. γ-Secretase inhibitor induces adipogenesis of adipose-derived stem cells by regulation of notch and PPAR-γ. cell Prolif. Wiley Online Library. 2010;43:147–56.

38. Andersen P, Uosaki H, Shenje LT, Kwon C. Non-canonical notch signaling: emerging role and mechanism. Trends Cell Biol Elsevier. 2012;22:257–65.

39. Sanalkumar R, Dhanesh SB, James J. Non-canonical activation of notch signaling/target genes in vertebrates. Cell Mol Life Sci Springer. 2010;67:2957–68.

40. Hayward P, Brennan K, Sanders P, Balayo T, DasGupta R, Perrimon N, et al. Notch modulates Wnt signalling by associating with Armadillo /β-catenin and regulating its transcriptional activity. Development The Company of Biologists Ltd. 2005;132:1819–30.